

Two Views Are Better than One: Monocular 3D Pose Estimation with Multiview Consistency

Christian Keilstrup Ingwersen¹, Rasmus Tirsgaard², Rasmus Nylander¹, Janus Nørtoft Jensen³, Anders Bjorholm Dahl², and Morten Rieger Hannemose²

¹ Trackman A/S

² Technical University of Denmark
cin@trackman.com

Abstract. Deducing a 3D human pose from a single 2D image or 2D keypoints is inherently challenging, given the fundamental ambiguity wherein multiple 3D poses can correspond to the same 2D representation. The acquisition of 3D data, while invaluable for resolving the pose ambiguity, is expensive and requires an intricate setup, often restricting its applicability to controlled lab environments. We improve the performance of deep learning-based monocular human pose estimation models by using multiview data but only during training. To do so we propose a novel loss function, *consistency loss*, that operates on two views and enables adding additional training data with only 2D supervision without knowing the camera’s intrinsic or extrinsic parameters. This loss enforces that the inferred 3D poses of an entire sequence from one view align with the inferred 3D poses from another view under a similarity transform. Our consistency loss substantially improves performance for fine-tuning with no available 3D data. Furthermore, we demonstrate that using our consistency loss can yield state-of-the-art performance when training models from scratch in a semi-supervised manner. Our experiments demonstrate that just two views offset by 90 degrees are enough to obtain good performance, with only marginal improvements by adding more views. Thus, we enable easy acquisition of domain-specific data by capturing activities with off-the-shelf cameras, eliminating the need for elaborate calibration procedures. This research opens new possibilities for domain adaptation in 3D pose estimation, providing a practical and cost-effective solution to customize models for specific applications. The used dataset, featuring additional views, will be made publicly available.

Keywords: 3D human pose · consistency loss · monocular 3D pose · semi-supervised

1 Introduction

Inferring a 3D human pose from a single 2D image or 2D keypoints is fundamentally an ambiguous problem, with a multiple of 3D poses having identical

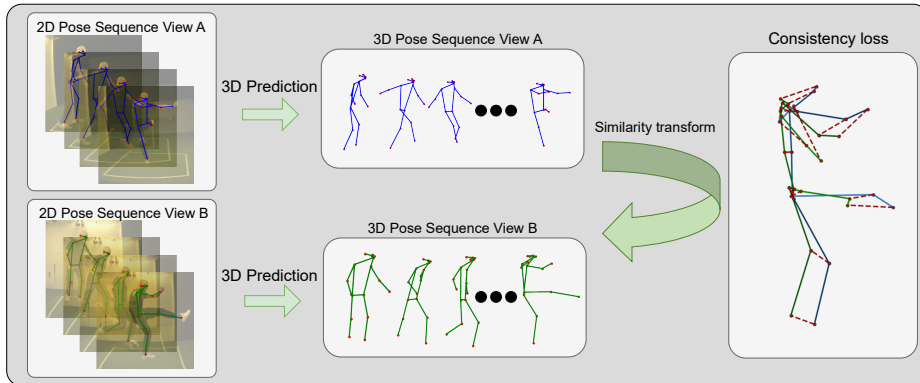


Fig. 1: We improve monocular performance by applying our consistency loss during training to predicted 3D pose sequences from two different views. The consistency loss penalizes variations between the two predicted pose sequences of the same activity. Note that we only use multiple views during training. For every predicted 3D pose sequence obtained from View A and View B, we compute a similarity transform with Procrustes Analysis. This transformation aligns the predicted poses in sequence A with sequence B. The consistency loss is the average distance in 3D between the two pose sequences post-alignment, shown as dashed red lines. Using Procrustes analysis for this transformation enables us to use cameras with unknown intrinsics and extrinsics.

2D representations. It is, however, possible to learn a mapping from a single 2D image to a 3D pose. Many methods rely either on 3D training data or on two or more views with a calibrated camera setup for training. We show how 3D pose can be accurately learned using only two synchronized uncalibrated cameras during training and still just a single 2D image for inference.

With this inherent ambiguity, models inferring 3D poses need an underlying representation of how the body can move and, ideally, which movements it can expect to see. To introduce such a prior in the model, it has become popular to rely on large foundation models [46], which have learned how the body moves in general. Even so, these do not always generalize to new movements or applications. This introduces the need for fine-tuning the foundation models to accommodate the less frequently seen movements specific for that domain [46].

Methods for adapting 3D human pose models to different domains and movements have traditionally relied on the availability of new 3D data [18, 44, 45]. However, it can be costly and may not be feasible to set up systems for capturing 3D data in the new domain. Alternative methods have been explored to address these challenges. These methods have demonstrated that 3D pose models can be fine-tuned using 2D data, as suggested by previous work [2]. This fine-tuning process ensures that the inferred 3D joint positions align with 2D keypoints in an image, which can be obtained accurately using readily available methods [16, 42]. Unfortunately, relying solely on 2D supervision from a single

view can cause models to forget their depth representation, which is problematic since we want to obtain an accurate 3D representation [11].

To advance fine-tuning with purely 2D supervision, we introduce a new loss function that enforces multiview consistency by requiring the inferred 3D pose from one view to be similar to the inferred 3D pose from another view under a similarity transform. Fig. 1 sketches the concept of our consistency loss.

While we focus on increasing the performance of monocular models and not models utilizing multiple views, many datasets used for training monocular models have multiple views of the scene available [12, 17, 29, 31]. We exploit this by utilizing the multiple views in the SportsPose [12] and Human3.6M [13] datasets to evaluate the feasibility of our loss. We demonstrate the improvements that can be obtained by using multiple views during training while only using a single view at inference time. Additionally, we investigate how many views are necessary to obtain improvements in 3D predictions. This study uses the SportsPose dataset [12], to demonstrate the performance of our proposed loss for fine-tuning a model to a model. The authors provided us access to all seven views of this dataset, which will be released together with this paper. The SportsPose dataset features complex and challenging sports scenarios, making it an ideal test bed for our domain-adaptive approach. The new views are available on our website³. Additionally, we demonstrate that our consistency loss can enhance model performance when training from scratch in a semi-supervised manner on the Human3.6M dataset. By utilizing our consistency loss, we obtain state-of-the-art among semi-supervised methods.

While we demonstrate our loss on the SportsPose dataset [12], which contains ground truth 3D data as well as a full multi-camera calibration, we only use the 3D data for evaluation, relying purely on predicted 2D keypoints for training. Because of the similarity transformation, our view-consistency loss eliminates the need for knowing the camera intrinsic or extrinsics, and only needs synchronized cameras. Foregoing camera calibration unlocks new opportunities for scaling multiview data acquisition as the footage can be captured on smartphones outside of the lab in diverse settings. The problem synchronization can be done with existing apps over WiFi [1] or solved as a post-processing step using audio cues [23].

Moreover, it resolves the inherent ambiguity associated with fine-tuning on 2D data. When using 2D data for training, the model can be confounded by multiple 3D points that project to the same 2D coordinates. Our multiview consistency loss provides a robust solution to this challenge, substantially enhancing the accuracy and reliability of monocular 3D pose estimation.

Our contributions extend beyond introducing the view-consistency loss for domain-adaptive 3D pose estimation. We also present the first set of baseline results on the SportsPose dataset, demonstrating the effectiveness of our approach. We illustrate how our method enhances 3D pose estimation accuracy in dynamic and complex environments by showcasing a model fine-tuned on the SportsPose dataset. This research opens up new possibilities for domain adaptation in 3D

³ Link removed for anonymity.

pose estimation, providing a practical and cost-effective solution to customize models for specific applications, and unlocks the possibility of increasing the state-of-the-art in monocular pose estimation by training on large amounts of two-view in the wild data.

2 Related work

2.1 Monocular 3D human pose models

Two primary approaches exist in the monocular 3D human pose estimation domain. One focuses solely on determining the 3D locations of the human skeleton [33, 38, 44], while the other includes estimating the body shape [2, 18, 21, 24, 43]. The latter category often employs parametric body models such as SMPL [27], which describes the body through shape parameters and pose parameters. Notably, our proposed loss remains applicable to both approaches, as 3D joint positions, as well as shape and pose parameters, can be penalized based on the variation between multiple views.

Irrespective of whether the goal is to estimate pose alone or to include shape parameters, monocular 3D human pose estimation commonly adopts either a one-stage or a two-stage approach. In one-stage approaches, the estimation is directly derived from an image or video input, while two-stage approaches involve lifting estimated 2D poses to 3D space. State-of-the-art monocular models that employ the two-stage approach, lifting 2D poses to 3D, achieve remarkable mean-per-joint precision errors (MPJPE [11]). They reach as low as 17mm [46] when lifting ground truth 2D poses on the Human3.6M dataset [13], and 37mm when lifting estimated 2D poses [46].

Models that adopt the alternative approach of inferring the 3D pose by estimating the parametric SMPL model directly from image input, have achieved MPJPE scores of 60mm [39] on the in-the-wild 3DPW dataset [28].

2.2 Multiview 3D human pose models and datasets

Multiple synchronized and calibrated cameras have been extensively used in human pose estimation work [4, 15, 34]. Utilizing calibrated camera setups in such approaches has yielded impressive results, even generating state-of-the-art 3D human pose datasets [12, 17, 29, 31]. These datasets, in turn, play a pivotal role in training and advancing monocular models. However, the practical implementation of multi-camera setups involves intricate calibration and synchronization processes, which often confines data to be collected in controlled laboratory environments.

Approaches that require limited or no 3D supervision have also been explored. Some of these are unsupervised and train on single images by lifting a 2D pose to 3D followed by a random rotation and re-projection to 2D [3, 6, 10, 41]. Others more similar to ours use multiple views of the same person [8, 14, 20, 26, 30]. Liu et al. [26] require a fully calibrated camera setup to predict poses. Others do

not require known extrinsics but estimate relative camera poses by decomposing the essential matrix estimated from 2D poses predicted in multiple views. Then, the 3D poses are triangulated using the estimated relative poses, which are then used as training data [8, 20]. Mitra et al. [30] add additional training data from multiview images and use metric learning to enforce that images of the same pose have similar embeddings. The approach of Iqbal et al. [14] is most similar to ours, but they require known camera intrinsic, and can only predict scale normalized poses. They infer 3D poses with a monocular model from multiple views and align them rigidly. During training, they penalize the model for differences in the predicted poses. However, the latter two approaches apply only multiview consistency on single image pairs and not sequences, thus significantly limiting their potential use.

3 Multiview consistency loss

Instead of relying on a known intrinsic or extrinsic calibration, our consistency loss can be deployed without any prior information about the cameras. Instead, the consistency loss applies a similarity transformation and penalizes differences in the poses of two sequences of the same activity, see Figure 1. Avoiding camera calibration simplifies the training pipeline and gives an efficient alternative for handling data from multiple views.

Specifically, the loss is based on the difference between poses computed from two or more views after alignment with a similarity transformation, τ . We compute the mean difference over every pair of two cameras, which results in the loss

$$\mathcal{L}_{\text{con}} = \sum_{s=1}^S \frac{1}{|V_s|} \sum_{(a,b) \in V_s} \mathcal{L}_c(\hat{J}_a, \hat{J}_b). \quad (1)$$

Here, S is the total number of sequences, and V_s is the set of possible pairs of views of the sequence s . Therefore, with N different cameras available in a sequence, $|V_s| = \binom{N}{2}$. The consistency loss \mathcal{L}_c is calculated between \hat{J}_a and \hat{J}_b , which are the predicted 3D body joints for all frames of the sequence from view a and view b , respectively. The term \mathcal{L}_c is

$$\mathcal{L}_c(\hat{J}_a, \hat{J}_b) = \frac{1}{n} \sum_{i=1}^n \left\| \tau(\hat{J}_{a,i}; \hat{\theta}_{ab}) - \hat{J}_{b,i} \right\|_2, \quad (2)$$

where $\hat{J}_{a,i}$ is element i , from the sequence of predicted 3D poses from view a , which has length n . Similarly, $\hat{J}_{b,i}$ is element i from the sequence of predicted 3D poses from view b . τ is a similarity transform with parameters $\hat{\theta}_{ab}$ that are estimated such that τ transforms $\hat{J}_{a,i}$ to be as close as possible to $\hat{J}_{b,i}$ by scaling, rotating, and translating the 3D joints from $\hat{J}_{a,i}$.

To compute the scaling, rotation, and translation used to transform $\hat{J}_{a,i}$, we estimate the optimal parameters $\hat{\theta}_{ab}$, as in Equation (3). Here, it should be noted

that contrary to how similarity transformations traditionally are computed in 3D human pose estimation to calculate the Procrustes aligned MPJPE, we only compute one transformation, $\hat{\theta}_{ab}$, for the entire sequence and not one per frame as in the PA-MPJPE metric [11].

$$\hat{\theta}_{ab} = \arg \min_{\theta} \sum_{i=1}^n \left\| \tau \left(\hat{J}_{a,i}; \theta \right) - \hat{J}_{b,i} \right\|_2^2. \quad (3)$$

The optimal solution to Equation (3) is found using Procrustes analysis [9], such that we obtain the optimal scaling, rotation, and translation to transform $\hat{J}_{a,i}$ as follows

$$\tau \left(\hat{J}_{a,i}; \hat{\theta}_{ab} \right) = s \hat{J}_{a,i} R + t. \quad (4)$$

By transforming \hat{J}_a , the idea is to directly estimate the similarity transformation that transforms from the camera coordinate system of camera a to the coordinate system of camera b instead of relying on knowing the camera extrinsics to perform the transformation.

4 Experiments

4.1 Test protocol

To evaluate our proposed consistency loss, as defined in Equation (1), we conduct experiments using the SportsPose dataset [12]. Since the original paper does not provide a specified test protocol, we employ a test protocol inspired by Human3.6M [13], wherein subjects are distributed across sets to ensure that no subject appears in the same set.

We use subjects S04, S07, S09, S14, and S22 for validation. Subsequently, we employ subjects S06, S12, and S19 for testing. To focus on monocular performance, we opt to use only the currently available view, “right”, during the testing and validation of the model. This decision streamlines the evaluation process, as we are interested in assessing the proficiency of the model when exposed to a single front-facing view. Examples of this view are in the first row of Figure 2.

4.2 Implementation

While our view-consistency loss is versatile and applicable to any monocular 3D human pose method, we choose to adapt the MotionBERT model by Zhu et al. [46] and fine-tuning it to the SportsPose [12] dataset.

To use SportsPose [12] with MotionBERT [46] we need to preprocess the data first. We convert the definition of body keypoints from COCO [25] keypoints used in SportsPose to the Human3.6M [13] body keypoint format. The keypoints are further transformed from meters to millimeters and, by using the extrinsic camera parameters, transformed from the world coordinate system to each camera. Then, following the approach in [5], the camera coordinates are transformed to pixel coordinates and scaled to be within the range $[-1; 1]$.

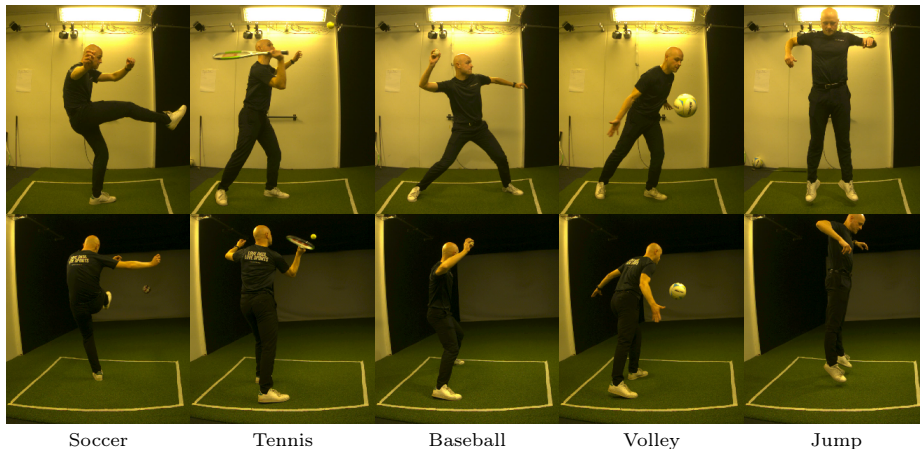


Fig. 2: The five activities from SportsPose [12]. The top row displays the publicly available view “right”. The bottom row features a view rotated 90 degrees relative to “right”, which we refer to as “View 1”.

For the fine-tuning of MotionBERT [46], we employ the weights provided for the DSTformer with a depth of five and eight heads. The sequence length is 243, and the feature and embedding sizes are 512. Adhering to the training protocol suggested by Zhu et al. [46], we fine-tune the models for 30 epochs, using a learning rate of 0.0002 and utilizing the Adam optimizer [19].

4.3 Fine-tuning with 3D data

To compare to the situation when 3D data is available, we also experiment with fine-tuning with 3D data. We implement the proposed fine-tuning configuration from MotionBERT. This involves using a positional loss, \mathcal{L}_{pos} directly on the 3D poses, coupled with losses on joint velocities, \mathcal{L}_{vel} , and scale only loss, $\mathcal{L}_{\text{scale}}$, as suggested by Rhodin et al. [35]. This combination results in the combined loss for 3D data,

$$\mathcal{L}_{3\text{D}} = \lambda_{\text{pos}}\mathcal{L}_{\text{pos}} + \lambda_{\text{vel}}\mathcal{L}_{\text{vel}} + \lambda_{\text{scale}}\mathcal{L}_{\text{scale}}, \quad (5)$$

where λ_{pos} , λ_{vel} , and λ_{scale} are weights for the respective losses. Our proposed consistency loss is added as a regularization term, $\lambda_{\text{con}}\mathcal{L}_{\text{con}}$, to the total loss, resulting in Equation (6),

$$\mathcal{L}_{3\text{D}_{\text{con}}} = \lambda_{\text{pos}}\mathcal{L}_{\text{pos}} + \lambda_{\text{vel}}\mathcal{L}_{\text{vel}} + \lambda_{\text{scale}}\mathcal{L}_{\text{scale}} + \lambda_{\text{con}}\mathcal{L}_{\text{con}}. \quad (6)$$

After an extensive parameter search, aligning with suggestions from Zhu et al. [46], we identify the optimal configuration for Equation (6) as $\lambda_{\text{pos}} = 1$, $\lambda_{\text{vel}} = 20$, $\lambda_{\text{scale}} = 0.5$, and $\lambda_{\text{con}} = 0.2$. These parameters are employed to obtain the results presented in Table 1, utilizing two camera views from SportsPose [12],

Table 1: Results on SportsPose [12]. Baseline is MotionBERT [46], which is then fine-tuned with either 2D (\mathcal{L}_{2D}) or 3D (\mathcal{L}_{3D}) supervision with and without our proposed multiview consistency loss \mathcal{L}_{con} . All results in mm, lower is better. MPJPE is mean per joint precision error, and PA is Procrustes aligned MPJPE. All results use predicted 2D poses [16]. **Bold** is the best performance with only 2D data and **bold gray** is best performance with 3D ground truth. The two views are in Figure 2. The consistency loss improves performance in both cases but substantially more when 3D supervision is not used.

	Soccer		Tennis		Baseball		Volley		Jumping		All	
	kick		serve		pitch							
	MPJPE	PA										
Baseline												
MotionBERT [46]	64.2	39.5	70.7	39.7	85.0	42.2	86.8	50.0	78.0	48.9	77.1	44.1
Iqbal <i>et al.</i> [14] ⁴	42.8	28.5	39.9	26.2	47.0	30.1	40.3	27.9	44.9	30.1	42.9	28.5
Fine-tuning with 3D data (2 views)												
\mathcal{L}_{3D} (5)	26.7	20.2	27.3	20.1	30.1	22.5	31.3	24.2	27.9	21.4	28.7	21.7
$\mathcal{L}_{3D_{con}}$ (6), Ours	26.1	20.5	25.4	18.8	29.4	22.4	30.8	23.8	27.9	20.9	28.0	21.3
Only 2D fine-tuning (2 views)												
\mathcal{L}_{2D} (7)	59.0	44.1	59.1	42.0	73.8	45.1	64.7	47.8	65.0	45.6	64.4	45.0
$\mathcal{L}_{2D_{con}}$ (8), Ours	36.6	22.5	34.2	22.2	41.7	25.2	37.3	23.7	32.0	22.7	36.4	22.0

one from the right side, as illustrated in the first row of Figure 2, and another 90 degrees to the view facing the back of the subject as in the second row of Figure 2. The second view behind the subject is based on the assumption that this view contains the most information when joints are occluding each other in the original “right” view from SportsPose [12].

The results in Table 1 show the impact of the consistency loss on model performance. Even when ground truth 3D data is available, the consistency loss yields marginal improvements, with a 0.8mm decrease in MPJPE and 0.2mm in PA-MPJPE. This slight enhancement suggests that our regularization term can be seamlessly integrated even when 3D data are available without compromising performance. It is crucial to emphasize that our consistency loss is intentionally crafted for scenarios lacking 3D data. But this underscores its utility as a valuable regularization technique for monocular pose estimation, acknowledging that the use of 3D data remains superior to achieve a well-performing model.

4.4 Fine-tuning without available 3D data

Refining a model through fine-tuning is still possible when ground truth 3D joint data are unavailable. This fine-tuning involves reprojecting the predicted 3D points onto the image and assessing how well these reprojected keypoints aligns

⁴ As they have not released their code, we re-implement an improved version of their method by incorporating MotionBERT as the backbone with sequence length 1.

with the ground truth 2D keypoints. However, obtaining precise ground truth 2D poses, although less challenging than gathering 3D poses and not requiring specialized hardware, requires substantial effort and manual annotation.

In practice, the use of ground truth 2D poses is limited due to annotation challenges. Instead, models frequently leverage estimated 2D keypoints from detectors such as HRNet [40], AlphaPose [7] or RTMPose [16] for supervision. Notably, when employing estimated keypoints, the reprojection error is often weighted by the confidence scores provided by the 2D keypoint detectors. This strategy minimizes the impact of less reliable keypoints on the overall training process while maintaining the essential guidance for model refinement.

To validate the performance of our proposed consistency loss, we use RTMPose [16] to predict 2D poses for all frames in the SportsPose dataset [12]. The predicted 2D poses are preprocessed as described in Section 4 and then used to fine-tune the MotionBERT [46] model. When fine-tuning the model without the consistency loss, we solely use the 2D reprojection loss,

$$\mathcal{L}_{2D} = \lambda_{2D_{\text{reproj}}} \mathcal{L}_{2D_{\text{reproj}}}. \quad (7)$$

Again we add the consistency loss as a regularization term resulting in the total loss in Equation (8). Through experimentation, we found that when two camera views are available, we achieve the best performance, with $\lambda_{2D_{\text{reproj}}} = 1$ and $\lambda_{\text{con}} = 0.3$,

$$\mathcal{L}_{2D_{\text{con}}} = \lambda_{2D_{\text{reproj}}} \mathcal{L}_{2D_{\text{reproj}}} + \lambda_{\text{con}} \mathcal{L}_{\text{con}}. \quad (8)$$

By fine-tuning the MotionBERT [46] model with the losses in Equations (7) and (8), using two camera views as described in Section 4.3, we achieve the results in Table 1.

The results in Tab. 1 highlight the impact of the consistency loss regularization term, particularly in scenarios where ground truth 3D information is absent. This regularization term leads to a substantial improvement in MPJPE, demonstrating a reduction of 39.2mm compared to relying solely on the reprojection loss. Visualizing 3D predictions from models with and without the consistency loss, Figure 3a, we see the same substantial increase in accuracy when using the consistency loss.

We believe this improvement is this big because the consistency loss has improved the network’s ability to resolve ambiguities during the process of lifting 2D to 3D from a single view. In addition, it proves beneficial in situations where joints might be occluded in one of the views, enhancing the overall robustness of the model.

However, a closer examination of the Procrustes aligned joint error in Table 1 reveals an interesting observation. Fine-tuning the model solely on 2D body keypoints results in an increase in error. This phenomenon could be attributed to the inherent ambiguity associated with multiple different 3D poses that can reproject to the same 2D body pose. Consequently, the model may struggle to provide accurate depth estimates of joint locations, as highlighted in the work by Ingwersen et al. [11]. This underscores the importance of the consistency

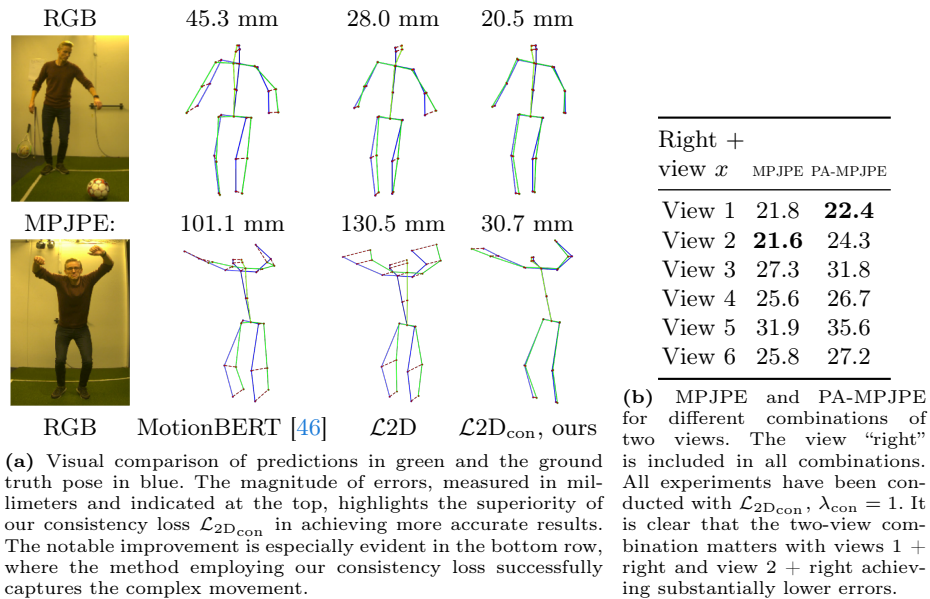


Fig. 3: **3a:** Visualization of the effect of our loss. **3b:** Overview of which views to use.

loss in mitigating such challenges and emphasizes its role in refining the model’s performance in the absence of ground truth 3D data.

4.5 Comparison with state-of-the-art on Human3.6M data

Table 2 shows results from our method with consistency loss compared with other semi-supervised methods trained on the Human3.6M [13] dataset. For the evaluation we adopt the same protocol as Iqbal *et al.* [14] using 3D supervision from subject (S1) and use other the subjects (S5, S6, S7, S8) for weak supervision with our consistency loss, $\mathcal{L}_{2D_{con}}$ from Eq. (8). For evaluation, we use the standard protocol testing on subjects S9 and S11 [13, 14].

The data depicted in Table 2 demonstrates that our novel consistency loss significantly improves performance in scenarios with limited 3D data with unlabeled multiview data. A key innovation of our approach, compared to Iqbal *et al.* [14], lies in incorporating the temporal aspect by computing a similarity transform per sequence instead of per frame, and not requiring known camera intrinsics. This advancement establishes a new state-of-the-art in semi-supervised performance on the Human3.6M dataset [13].

4.6 How many views do we need?

Examining the experiments carried out in Sections 4.3 and 4.4, a logical inquiry arises regarding the scalability of the results when more than two views are

Table 2: Comparison with state-of-the-art Semi-Supervised methods on the Human3.6M [13] dataset using only 3D data from Subject 1 for training.

Methods	MPJPE ↓	PA-MPJPE ↓
Rodhin et al. (ECCV'18) [35]	131.7	98.2
Pavlakos et al. (ICCV'19) [32]	110.7	74.5
Li et al. (ICCV'19) [22]	88.8	66.5
Rodhin et al. (CVPR'18) [36]	-	65.1
Kocabas et al. (CVPR'19) [20]	-	60.2
Iqbal et al. (CVPR'20) [14]	62.8	51.4
Roy et al. (3DV'22) [37]	60.8	48.4
Ours	58.9	43.6

incorporated into the experiments. To investigate the correlation between the number of views and performance, we have calculated the results for scenarios where one to seven views are available, encompassing the total number of views in the SportsPose dataset [12].

Without available 3D data. In the absence of ground-truth 3D data, the influence of including multiple views on accuracy is evident as shown in Section 4.4 and the results in Table 1. To compute the results that involve more than two views without access to 3D data, we utilize the loss function from Equation (8) with a consistent configuration, specifically setting $\lambda_{2D_{reproj}} = 1$ and $\lambda_{con} = 1$ for all experiments. It is essential to note that this configuration is not fine-tuned for a specific number of views, which may result in variations compared to the results presented in Table 1. The outcome of this ablation study is detailed in Figure 4a.

Examining the results for 2D supervision in Figure 4a reveals a substantial increase in accuracy as we progress from one to two views. However, the accuracy curve for both MPJPE and PA-MPJPE appears to plateau beyond two views, with marginal gains observed when incorporating more than two views.

This observed plateau could be attributed to diminishing returns in information gain beyond the second view. While additional views contribute valuable perspectives, they may not necessarily introduce new information that significantly refines the precision of the predicted joints. Interestingly, this property of the loss underscores its utility, particularly in scenarios where capturing new data becomes significantly more manageable requiring only two views of the activity from an uncalibrated camera setup.

With available 3D data. Even when 3D data is available, incorporating our consistency loss with two views results in a modest performance gain in MPJPE or PA-MPJPE, as illustrated in Section 4.3 and detailed in Table 1. This raises the question of whether this incremental gain will persist with an increasing number of views or reach a plateau, similar to the findings with only 2D. In these experiments, we employ the loss function from Equation (6) with $\lambda_{pos} = 1$, $\lambda_{vel} = 20$, $\lambda_{scale} = 0.5$, and $\lambda_{con} = 1$. Notably, these values are not fine-tuned for any specific number of views and may thus differ from the results presented

in Table 1. The outcomes of this experiment are illustrated in Figure 4b. We observe a slight increase in performance when additional views are added, along with the inclusion of our consistency loss. However, the variation in performance is generally small, and the overarching conclusion remains unchanged: when 3D data is available, there is no need to adapt the consistency loss.

4.7 More views or more data?

Examining Figures 4a and 4b, one may question if both the marginal accuracy improvements for 3D supervision and the substantial gains with 2D supervision with our consistency loss are only due to the increased amount of training data. To explore this we have conducted the same experiments but without including \mathcal{L}_{con} in the loss.

In the experiment analogous to 2D supervision illustrated in Figure 4a, an examination of the results without the consistency loss in Figure 4c reveals that neither MPJPE nor PA-MPJPE exhibit improvement with the addition of more training data through an increased number of views. The observed plateau after two views contradicts the substantial accuracy increases depicted in Figure 4a, suggesting that these improvements are attributed to the introduction of our consistency loss.

However, examining the experiments adding data to the 3D supervision in Figure 4d, we observe a trend similar to that depicted in Figure 4b with the error decreasing marginally when we add more data to the training. This suggests that the marginal improvements in accuracy when employing our consistency loss with 3D supervision can be attributed to the increased volume of data rather than solely to the presence of the consistency loss. This finding supports the overarching conclusion that 3D data is superior, and supports that the main advantage of our consistency loss lies in enhancing accuracy in scenarios where obtaining 3D data is impractical.

4.8 Which views to choose

In the experiments of Figures 4a and 4b, the selection of views followed a deterministic process. Specifically, the first view was consistently chosen as the “right” view from SportsPose [12], and the second view was facing the back of the subject i.e. the one positioned closest to a 90-degree angle relative to the initial view. For scenarios involving three or more views, the remaining views were selected arbitrarily but maintained the same order across all experiments.

As the ambiguities of a 3D pose can theoretically be solved when observing from any two different views, a question arises if there is a practical advantage of certain viewpoints. This was investigated in Figure 3b where the model was trained using the “right” view in combination with all other available views, where View 1 corresponds to the perspective positioned 90 degrees relative to the view facing the back of the subject.

Analyzing the errors depicted in Figure 3b, it is evident that the choice of the view for multiview supervision significantly influences the outcomes of using our

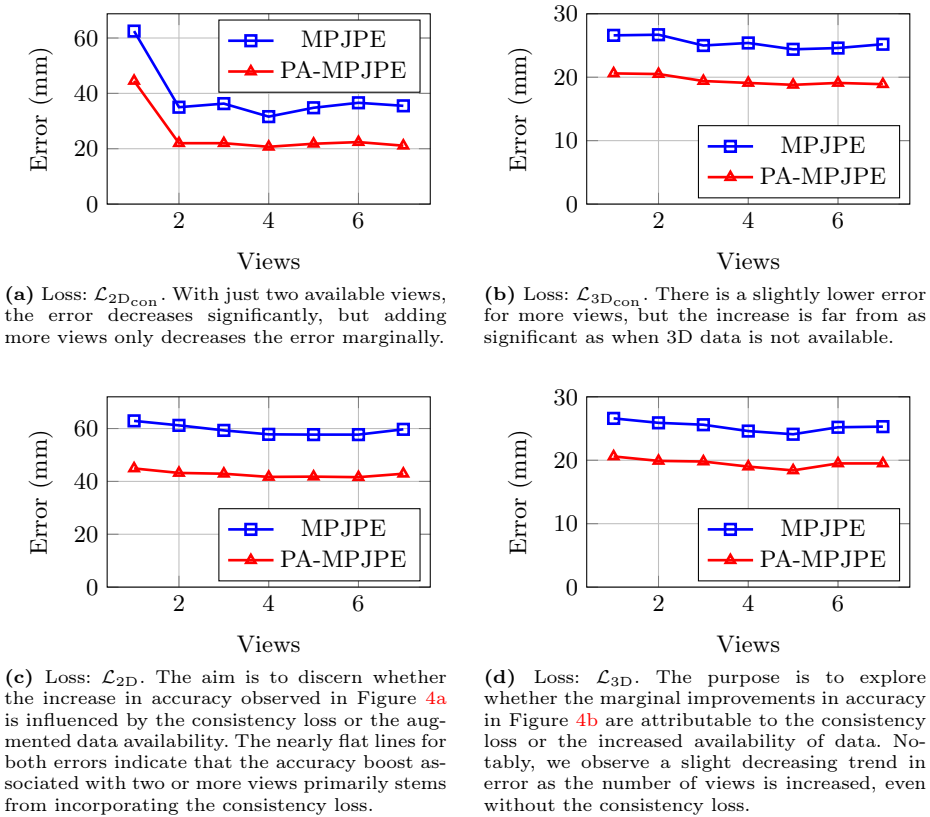


Fig. 4: Investigation of how MPJPE and PA-MPJPE are affected when varying the number of views available with different losses. Top: With consistency loss, $\lambda_{con} = 1$, bottom without consistency loss. Left: 2D, right: 3D.

consistency loss. This aligns with intuition, as certain views are more effective in resolving ambiguities and identifying occluded joints, while others may not contribute new information. The results indicate that an optimal configuration involves using views from two sides that are 90 degrees apart when only two cameras are available.

5 Discussion and conclusion

Limitations. While our results underscore a notable improvement in accuracy achieved through the implementation of our consistency loss, it is important to acknowledge the limitations of our method. As Figure 3b demonstrates, the effect of the consistency loss is dependent on which views are used during training, with the least favorable combination resulting in performance comparable to using a

single camera view. However, a substantial increase in accuracy is evident in four out of five combinations.

Furthermore, it is essential to highlight that an excessive emphasis on the consistency loss, indicated by a large λ_{con} value, can lead to a degenerate solution. Specifically, an optimal solution to Equation (2) may manifest as predicting an identical position of all joints, emphasizing the need for careful consideration when setting this parameter.

Our proposed consistency loss estimates a single transformation for a pose sequence for aligning the 3D poses from different views. While this requires the cameras to be stationary throughout the sequence, our method can be extended to movable cameras by finding a similarity transformation for each time step.

It is worth noting that incorporating the proposed consistency loss necessitates temporal synchronization of pose sequences from different views. Desynchronization will appear as correlated noise in the 2D predictions that in the worst case can confuse the model, especially for fast movements. This requirement imposes constraints on the camera system used for data capture. Using two cameras capturing frames with logged timestamps, it is possible to manually identify the same point in time in both sequences, or to use the audio to time-synchronize the views after acquisition [23]. However, if using Android smartphones as cameras the frame-synchronization can be obtained using an app and WiFi hotspots as described by Akhmetyanov *et al.* [1].

Conclusion. We present a novel method to enhance monocular 3D human pose estimation performance. By incorporating our multiview consistency loss during training in scenarios where 3D data is unavailable, we achieve notable performance improvements when compared to relying solely on a 2D reprojection loss or no fine-tuning without requiring knowledge of the camera’s extrinsic or intrinsic parameters.

We demonstrate the efficacy of the proposed consistency loss by evaluating it on the Human3.6M [13] and SportsPose [12] dataset. Following the semi-supervised protocol for Human3.6M, we advance the precision and achieve state-of-the-art precision.

A thorough analysis exploring various configurations involving the number of views and camera placement reveals that an effective enhancement is achieved with just two appropriately positioned views. We observe that positioning the cameras at a 90-degree angle yields consistently good performance compared to other combinations of views. This demonstrates that, through the use of our multiview consistency loss, it is feasible to capture new domain data for fine-tuning a 3D model with a simple setup needing only two appropriately positioned and time-synchronized cameras.

With this paper, we also release six new views of sports activities to the SportsPose [12] dataset. Together with the new data we propose a new test protocol for the dataset and provide a simple baseline relying on MotionBERT [46] and our proposed consistency loss.

References

1. Akhmetyanov, A., Kornilova, A., Faizullin, M., Pozo, D., Ferrer, G.: Sub-millisecond video synchronization of multiple android smartphones. 2021 IEEE Sensors pp. 1–4 (2021), <https://api.semanticscholar.org/CorpusID:235727571> 3, 14
2. Bogo, F., Kanazawa, A., Lassner, C., Gehler, P., Romero, J., Black, M.J.: Keep it SMPL: Automatic estimation of 3D human pose and shape from a single image. In: Computer Vision – ECCV 2016. Lecture Notes in Computer Science, Springer International Publishing (Oct 2016) 2, 4
3. Chen, C.H., Tyagi, A., Agrawal, A., Drover, D., Mv, R., Stojanov, S., Rehg, J.M.: Unsupervised 3d pose estimation with geometric self-supervision. In: Proceedings of the IEEE/CVF conference on computer vision and pattern recognition. pp. 5714–5724 (2019) 4
4. Chun, S., Park, S., Chang, J.Y.: Representation learning of vertex heatmaps for 3d human mesh reconstruction from multi-view images (2023) 4
5. Ci, H., Ma, X., Wang, C., Wang, Y.: Locally connected network for monocular 3d human pose estimation. IEEE Transactions on Pattern Analysis and Machine Intelligence 44(3), 1429–1442 (2020) 6
6. Drover, D., MV, R., Chen, C.H., Agrawal, A., Tyagi, A., Phuoc Huynh, C.: Can 3d pose be learned from 2d projections alone? In: Proceedings of the European Conference on Computer Vision (ECCV) Workshops. pp. 0–0 (2018) 4
7. Fang, H.S., Li, J., Tang, H., Xu, C., Zhu, H., Xiu, Y., Li, Y.L., Lu, C.: Alphapose: Whole-body regional multi-person pose estimation and tracking in real-time. IEEE Transactions on Pattern Analysis and Machine Intelligence (2022) 9
8. Gholami, M., Rezaei, A., Rhodin, H., Ward, R., Wang, Z.J.: Tripose: A weakly-supervised 3d human pose estimation via triangulation from video. arXiv preprint arXiv:2105.06599 (2021) 4, 5
9. Gower, J.C.: Generalized procrustes analysis. Psychometrika 40(1), 33–51 (1975). <https://doi.org/10.1007/BF02291478> 6
10. Hardy, P., Kim, H.: Links" lifting independent keypoints"-partial pose lifting for occlusion handling with improved accuracy in 2d-3d human pose estimation. In: Proceedings of the IEEE/CVF Winter Conference on Applications of Computer Vision. pp. 3426–3435 (2024) 4
11. Ingwersen, C.K., Jensen, J.N., Hannemose, M.R., Dahl, A.B.: Evaluating current state of monocular 3d pose models for golf. In: Proceedings of the Northern Lights Deep Learning Workshop. vol. 4 (2023). <https://doi.org/https://doi.org/10.7557/18.6793> 3, 4, 6, 9
12. Ingwersen, C.K., Mikkelsen, C., Jensen, J.N., Hannemose, M.R., Dahl, A.B.: Sportspose: A dynamic 3d sports pose dataset. In: Proceedings of the IEEE/CVF International Workshop on Computer Vision in Sports (2023) 3, 4, 6, 7, 8, 9, 11, 12, 14
13. Ionescu, C., Papava, D., Olaru, V., Sminchisescu, C.: Human3.6m: Large scale datasets and predictive methods for 3d human sensing in natural environments. IEEE Transactions on Pattern Analysis and Machine Intelligence 36(7), 1325–1339 (jul 2014) 3, 4, 6, 10, 11, 14
14. Iqbal, U., Molchanov, P., Kautz, J.: Weakly-supervised 3d human pose learning via multi-view images in the wild. In: Proceedings of the IEEE/CVF conference on computer vision and pattern recognition. pp. 5243–5252 (2020) 4, 5, 8, 10, 11

15. Isakov, K., Burkov, E., Lempitsky, V., Malkov, Y.: Learnable triangulation of human pose. In: International Conference on Computer Vision (ICCV) (2019) [4](#)
16. Jiang, T., Lu, P., Zhang, L., Ma, N., Han, R., Lyu, C., Li, Y., Chen, K.: RTM-Pose: Real-Time Multi-Person Pose Estimation based on MMPose. arXiv e-prints arXiv:2303.07399 (Mar 2023). <https://doi.org/10.48550/arXiv.2303.07399> [2](#), [8](#), [9](#)
17. Joo, H., Liu, H., Tan, L., Gui, L., Nabbe, B., Matthews, I., Kanade, T., Nobuhara, S., Sheikh, Y.: Panoptic studio: A massively multiview system for social motion capture. In: 2015 IEEE International Conference on Computer Vision (ICCV). IEEE (dec 2015). <https://doi.org/10.1109/iccv.2015.381>, <https://doi.org/10.1109/iccv.2015.381> [3](#), [4](#)
18. Kanazawa, A., Black, M.J., Jacobs, D.W., Malik, J.: End-to-end recovery of human shape and pose. In: 2018 IEEE/CVF Conference on Computer Vision and Pattern Recognition. pp. 7122–7131 (2018). <https://doi.org/10.1109/CVPR.2018.00744> [2](#), [4](#)
19. Kingma, D.P., Ba, J.: Adam: A method for stochastic optimization. arXiv preprint arXiv:1412.6980 (2014) [7](#)
20. Kocabas, M., Karagoz, S., Akbas, E.: Self-supervised learning of 3d human pose using multi-view geometry. In: Proceedings of the IEEE/CVF conference on computer vision and pattern recognition. pp. 1077–1086 (2019) [4](#), [5](#), [11](#)
21. Kolotouros, N., Pavlakos, G., Black, M., Daniilidis, K.: Learning to reconstruct 3d human pose and shape via model-fitting in the loop. In: 2019 IEEE/CVF International Conference on Computer Vision (ICCV). pp. 2252–2261 (2019). <https://doi.org/10.1109/ICCV.2019.00234> [4](#)
22. Li, Z., Wang, X., Wang, F., Jiang, P.: On boosting single-frame 3d human pose estimation via monocular videos. In: Proceedings of the IEEE/CVF international conference on computer vision. pp. 2192–2201 (2019) [11](#)
23. Liang, J., Huang, P., Chen, J., Hauptmann, A.: Synchronization for multi-perspective videos in the wild. In: 2017 IEEE International Conference on Acoustics, Speech and Signal Processing (ICASSP). pp. 1592–1596. IEEE (2017) [3](#), [14](#)
24. Lin, K., Wang, L., Liu, Z.: End-to-end human pose and mesh reconstruction with transformers. In: 2021 IEEE/CVF Conference on Computer Vision and Pattern Recognition (CVPR). pp. 1954–1963 (2021). <https://doi.org/10.1109/CVPR46437.2021.00199> [4](#)
25. Lin, T., Maire, M., Belongie, S.J., Bourdev, L.D., Girshick, R.B., Hays, J., Perona, P., Ramanan, D., Dollár, P., Zitnick, C.L.: Microsoft COCO: common objects in context. CoRR [abs/1405.0312](https://arxiv.org/abs/1405.0312) (2014), <http://arxiv.org/abs/1405.0312> [6](#)
26. Liu, Y., Cheng, X., Ikenaga, T.: Motion-aware and data-independent model based multi-view 3d pose refinement for volleyball spike analysis. *Multimedia Tools and Applications* pp. 1–24 (2023) [4](#)
27. Loper, M., Mahmood, N., Romero, J., Pons-Moll, G., Black, M.J.: SMPL: A skinned multi-person linear model. *ACM Trans. Graphics (Proc. SIGGRAPH Asia)* **34**(6), 248:1–248:16 (Oct 2015) [4](#)
28. von Marcard, T., Henschel, R., Black, M., Rosenhahn, B., Pons-Moll, G.: Recovering accurate 3d human pose in the wild using imus and a moving camera. In: European Conference on Computer Vision (ECCV) (sep 2018) [4](#)
29. Mehta, D., Rhodin, H., Casas, D., Fua, P., Sotnychenko, O., Xu, W., Theobalt, C.: Monocular 3d human pose estimation in the wild using improved cnn supervision. In: 2017 International Conference on 3D Vision (3DV). pp. 506–516 (2017). <https://doi.org/10.1109/3DV.2017.00064> [3](#), [4](#)

30. Mitra, R., Gundavarapu, N.B., Sharma, A., Jain, A.: Multiview-consistent semi-supervised learning for 3d human pose estimation. In: Proceedings of the IEEE/CVF conference on computer vision and pattern recognition. pp. 6907–6916 (2020) [4](#), [5](#)
31. Nibali, A., Millward, J., He, Z., Morgan, S.: ASPset: An outdoor sports pose video dataset with 3d keypoint annotations. Image and Vision Computing **111**, 104196 (jul 2021). <https://doi.org/10.1016/j.imavis.2021.104196>, <https://doi.org/10.1016/j.imavis.2021.104196> [3](#), [4](#)
32. Pavlakos, G., Kolotouros, N., Daniilidis, K.: Texturepose: Supervising human mesh estimation with texture consistency. In: Proceedings of the IEEE/CVF International Conference on Computer Vision. pp. 803–812 (2019) [11](#)
33. Pavlo, D., Feichtenhofer, C., Grangier, D., Auli, M.: 3d human pose estimation in video with temporal convolutions and semi-supervised training. In: Conference on Computer Vision and Pattern Recognition (CVPR) (2019) [4](#)
34. Reddy, N.D., Guigues, L., Pishchulin, L., Eledath, J., Narasimhan, S.G.: Tesstrack: End-to-end learnable multi-person articulated 3d pose tracking. In: Proceedings of the IEEE/CVF Conference on Computer Vision and Pattern Recognition (CVPR). pp. 15190–15200 (June 2021) [4](#)
35. Rhodin, H., Salzmann, M., Fua, P.: Unsupervised geometry-aware representation learning for 3d human pose estimation. In: ECCV (2018) [7](#), [11](#)
36. Rhodin, H., Spörri, J., Katircioglu, I., Constantin, V., Meyer, F., Müller, E., Salzmann, M., Fua, P.: Learning monocular 3d human pose estimation from multi-view images. In: Proceedings of the IEEE conference on computer vision and pattern recognition. pp. 8437–8446 (2018) [11](#)
37. Roy, S., Citraro, L., Honari, S., Fua, P.: On triangulation as a form of self-supervision for 3d human pose estimation. In: 2022 International Conference on 3D Vision (3DV). pp. 1–10. IEEE Computer Society, Los Alamitos, CA, USA (sep 2022). <https://doi.org/10.1109/3DV57658.2022.00068>, <https://doi.ieeeecomputersociety.org/10.1109/3DV57658.2022.00068> [11](#)
38. Shan, W., Liu, Z., Zhang, X., Wang, S., Ma, S., Gao, W.: P-stmo: Pre-trained spatial temporal many-to-one model for 3d human pose estimation. In: Computer Vision–ECCV 2022: 17th European Conference, Tel Aviv, Israel, October 23–27, 2022, Proceedings, Part V. pp. 461–478. Springer (2022) [4](#)
39. Shetty, K., Birkhold, A., Jaganathan, S., Strobel, N., Kowarschik, M., Maier, A., Egger, B.: Pliks: A pseudo-linear inverse kinematic solver for 3d human body estimation. In: Proceedings of the IEEE/CVF Conference on Computer Vision and Pattern Recognition (CVPR). pp. 574–584 (June 2023) [4](#)
40. Sun, K., Xiao, B., Liu, D., Wang, J.: Deep high-resolution representation learning for human pose estimation. In: Proceedings of the IEEE/CVF conference on computer vision and pattern recognition. pp. 5693–5703 (2019) [9](#)
41. Wandt, B., Little, J.J., Rhodin, H.: Elepose: Unsupervised 3d human pose estimation by predicting camera elevation and learning normalizing flows on 2d poses. In: Proceedings of the IEEE/CVF Conference on Computer Vision and Pattern Recognition. pp. 6635–6645 (2022) [4](#)
42. Wang, J., Sun, K., Cheng, T., Jiang, B., Deng, C., Zhao, Y., Liu, D., Mu, Y., Tan, M., Wang, X., Liu, W., Xiao, B.: Deep high-resolution representation learning for visual recognition. Ieee Transactions on Pattern Analysis and Machine Intelligence **43**(10), 3349–3364 (2021). <https://doi.org/10.1109/TPAMI.2020.2983686> [2](#)
43. Xu, H., Bazavan, E.G., Zanfir, A., Freeman, W.T., Sukthankar, R., Sminchisescu, C.: Ghum & ghuml: Generative 3d human shape and articulated pose models. In: Proceedings of the IEEE/CVF Conference on Computer Vision and Pattern Recognition. pp. 6184–6193 (2020) [4](#)

44. Zhang, J., Tu, Z., Yang, J., Chen, Y., Yuan, J.: Mixste: Seq2seq mixed spatio-temporal encoder for 3d human pose estimation in video. In: Proceedings of the IEEE/CVF Conference on Computer Vision and Pattern Recognition (CVPR). pp. 13232–13242 (June 2022) [2](#), [4](#)
45. Zheng, C., Zhu, S., Mendieta, M., Yang, T., Chen, C., Ding, Z.: 3d human pose estimation with spatial and temporal transformers. In: Proceedings of the IEEE/CVF International Conference on Computer Vision (ICCV). pp. 11656–11665 (October 2021) [2](#)
46. Zhu, W., Ma, X., Liu, Z., Liu, L., Wu, W., Wang, Y.: Motionbert: A unified perspective on learning human motion representations. In: Proceedings of the IEEE/CVF International Conference on Computer Vision (2023) [2](#), [4](#), [6](#), [7](#), [8](#), [9](#), [10](#), [14](#)